

Optical properties of ZnS nanoparticles produced by mechanochemical method

C.S. Pathak^a, D.D. Mishra^{b,*}, V. Agarwala^b, M.K. Mandal^a

^aDepartment of Physics, National Institute of Technology, Durgapur 713209, India

^bDepartment of Metallurgical and Materials Engineering, Indian Institute of Technology, Roorkee 247667, India

Received 2 April 2012; received in revised form 20 April 2012; accepted 21 April 2012

Available online 3 May 2012

Abstract

Nanosized zinc sulfide (ZnS) has been synthesized by the mechanochemical route using zinc acetate and sodium sulfide as source materials in a high energy planetary ball mill (HEPBM) with 300 rpm for 2 h. The mechanochemically synthesized powders have been analyzed by X-ray diffraction (XRD) for phase analysis, Field Emission Scanning Electron Microscope (FESEM) for the morphological characterization, UV–vis–NIR spectrophotometer for determining band gap energy and Fluorescence spectroscopy for determining the emission wavelength. The crystallite size of the synthesized ZnS nanoparticles calculated by the Debye–Scherer's formula is in the range 7–9 nm. FESEM morphology shows the fibrous structure of ZnS samples. The value of optical band gap has been found to be in the range 5.2–5.3 eV. Room temperature photoluminescence (PL) spectrum of the samples exhibits a blue light emission using UV excitation wavelength of 280 nm.

© 2012 Elsevier Ltd and Techna Group S.r.l. All rights reserved.

Keywords: C. Optical properties; Semiconductors; Nanoparticles; Mechanochemistry

1. Introduction

Nanosized semiconductor particles especially II–VI semiconductors have attracted great deal of attention in the past few decades due to their unique properties and potential applications. Zinc sulfide semiconductor material has been studied for a variety of applications, including light-emitting diodes, electroluminescence, flat panel displays, infrared windows, lasers, biodevices, optical coating, electro-optic modulator, photoconductors, optical sensors, phosphors etc. [1]. In the past few decades the optical properties of the nanocrystalline semiconductors have been studied extensively [2–5]. Nanocrystalline semiconductors behave differently from bulk semiconductors. The band structure, band gap changes due to decrease in particle size, the band gap increases with the edges of the band split into discrete energy levels. Quantum-confinement effects have attracted great interest in basic and applied research

[6,7]. Semiconductor nanoparticle can be obtained from various methods such as a spray-based method [8], mechano-chemical route [9–11], ultrasonic radiation method [12], chemical precipitation method [13–15], electro spinning technique [16] and sol–gel method etc. [17]. In mechanochemical process, chemical reaction and phase transformation take place due to application of mechanical energy [18].

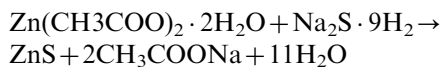
In this paper we reported the optical properties of ZnS nanoparticles milled for 2 h using mechanochemical route at room temperature. The mechanochemical technique is a useful technique as the main advantage of the process is permitting large quantities of nano materials to be produced at room temperature in a very short processing time [19]. We can also control the particle size by changing the milling condition and the starting materials. Repeated welding and fracture of reacting particle during ball-powder collision are the main characteristics of mechanochemical reactions. The milled powder consists of nano composite mixture of product phase. A washing process simply removes the by-product phase yields the desired phase.

*Corresponding author. Tel.: +91 9045760978; fax: +91 1332285738.

E-mail addresses: debeshmaterials@gmail.com,
debbsdmt@iitr.ernet.in (D.D. Mishra).

2. Experimental procedure

Zinc acetate (Merck, AR grade), sodium sulfide (Merck, AR grade) stoichiometric powder mixtures were prepared and milled in Retsch PM 400/2 planetary ball mill in order to prepare approximately 3 g of ZnS. The reaction occurring during the milling is given in Eq. (1).



The ball to powder weight ratio (BPR) was 5:1. The milling was performed in a (Retsch PM 400/2) ball mill for 2 h at a milling speed of 300 rpm and vial rotation speed of 600 rpm. Milling parameters are shown in Table 1.

ZnS nanoparticle can be obtained by washing the unreacted precursors and soluble product. The simple procedure for nanoparticles generation is milling and their separation, washing and heat treatment steps. Removal of impurity from the as milled powder was carried out with methanol using centrifuge (Remi PR 24) for 5 min at 10000 rpm, and washed with methanol several times to remove all sodium particle. The washed powder was then heat treated at 100 °C, 200 °C and 300 °C for 1 h.

The samples were characterized by means of X-ray diffraction (XRD) using a D8 BRUKER AXS diffractometer with Cu K α , operating at 40 kV and 30 mA. The crystallite size of the as-milled powders was determined by X-ray line broadening and calculated using the Scherrer equation:

$$D = \frac{0.9\lambda}{\beta \cos \theta} \quad (2)$$

where $\beta = (\beta_M^2 - \beta_I^2)^{1/2}$, β_M is the full width at half maximum (FWHM), β_I is the correction factor for instrument broadening, θ is the angle of the peak maximum, and λ is the Cu K α weighted wavelength ($=0.15406$ nm).

The morphological characteristics were analyzed using a QUANTA FEI-200 Field emission scanning electron microscope (FESEM). Energy-dispersive analysis of X-rays (EDAX) coupled with FESEM was used for the semi-quantitative investigation of the microstructure of the samples. Absorption spectra of the samples dispersed in methanol are studied with the help of UV–vis–NIR Spectrophotometer (Varian Cary 5000). The PL spectrum of the ZnS has been measured at room temperature using a Hitachi RF-5301 PC Spectrophotometer.

Table 1
Milling parameters.

Planetary ball mill details (Retsch PM 400/2)	Milling parameters
Milling Balls—Hardened steel balls	Milling Atmosphere—Air
Milling Jars—Hardened steel jars	Ball to powder ratio—5:1
Jar capacity—500 ml	Milling speed—300 rpm
	Vial Speed—600 rpm
	Total time of milling—2 h
	Weight of initial charge—15 g

3. Results and discussion

3.1. X-ray diffraction pattern

XRD patterns of the prepared ZnS samples at different heat treatment temperature were obtained and these are shown in Fig. 1. Fig. 1 shows the three diffraction peaks at 2θ values 28.6°, 47.7° and 56.3°. The peaks are appearing due to reflection from the (111), (220) and (311) planes of the cubic phase of the ZnS. The obtained peak positions correspond to zinc blended type patterns for all the samples. The XRD pattern of the nanocrystal is well matched with the standard cubic ZnS. The broadening of the XRD pattern of the prepared ZnS sample takes place due to the nanocrystalline nature of the sample. The crystallite size of the synthesized ZnS nanoparticles is found in the range 7–9 nm as calculated by using Eq. (2).

We can conclude that the nanocrystallite growth rate is different in different temperature due to interfacial reaction during heat treatment. The crystallite size of ZnS nanoparticles calculated by using the Scherrer equation is plotted as a function of heat treatment temperature as shown in Fig. 2. From Fig. 2 we can easily see that the crystallite size increased slowly with heat treating temperature from 7 to 9 nm.

3.2. FESEM analyses

Fig. 3 shows the FESEM images of the ZnS nanoparticles. FESEM morphology of the samples shows the fine fibrous structure for the sample which is heat treated at 100 °C for 1 h and becomes agglomerated with increasing heat treatment temperatures. The actual size cannot be determined by FESEM due to the limitations of the resolutions of the instrument.

Fig. 4 shows the EDAX spectrum, strong peaks of Zn and S are found in the EDAX spectrum. This confirmed the composition of ZnS sample.

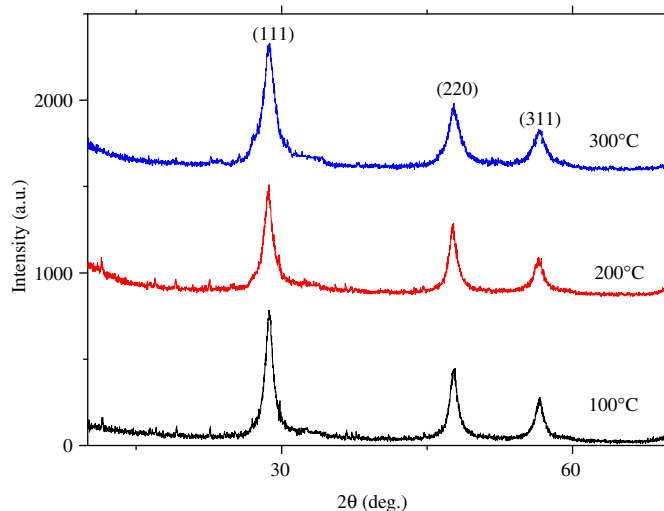


Fig. 1. XRD patterns of ZnS nanoparticles milled for 2 h and heat treated at different temperatures for 1 h.

3.3. Optical absorption and optical band gap

The optical absorption spectra are shown in Fig. 5. For measuring the absorption characteristics, the nanopowders are first dispersed in methanol and then taken in a quartz cuvette.

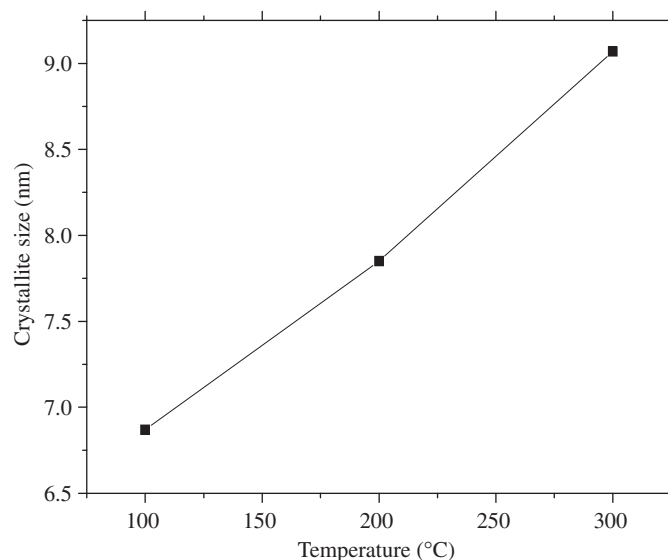


Fig. 2. Variations of crystallite size with different heat treating temperatures for 1 h.

From the optical absorption spectra of ZnS nanoparticles it is clear that optical absorption spectra of ZnS nanoparticles appear in the wavelength range 250–350 nm and this peak position reflects the band gap of particles. There is no absorption peak at visible region (400–800 nm). The fundamental absorption, which corresponds to electron excitation from the valance band to the

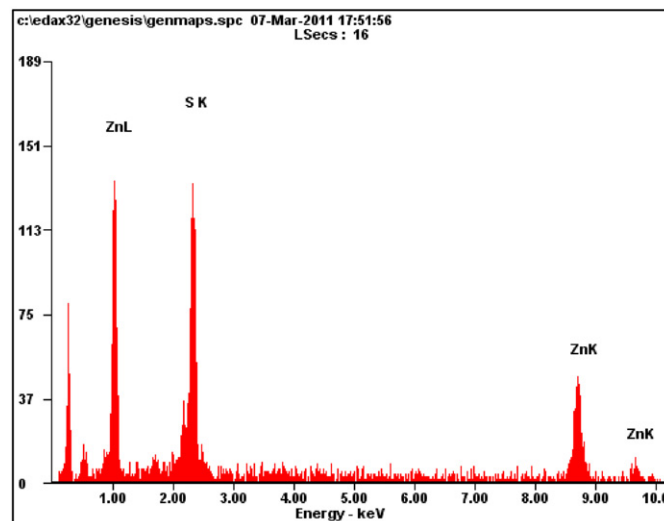


Fig. 4. EDAX spectrum of ZnS nanoparticles.

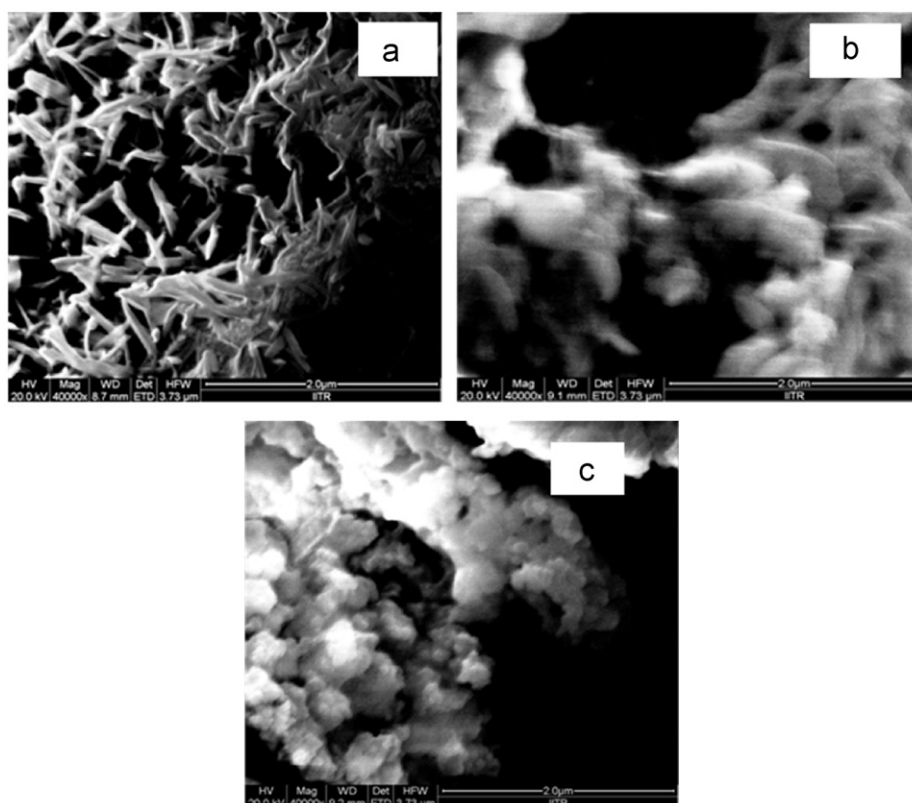


Fig. 3. FESEM images of ZnS nanoparticles heat treated for 1 h at (a) 100 °C, (b) 200 °C and (c) 300 °C.

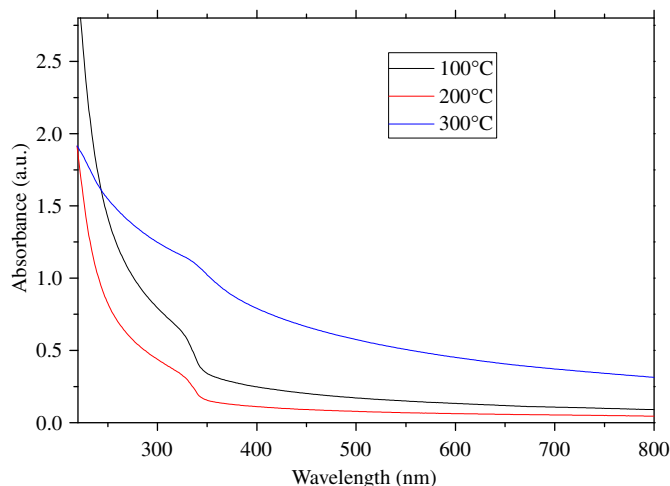


Fig. 5. UV-vis-NIR absorption characteristics of the prepared ZnS nanoparticles heat treated at 100 °C, 200 °C and 300 °C respectively for 1 h.

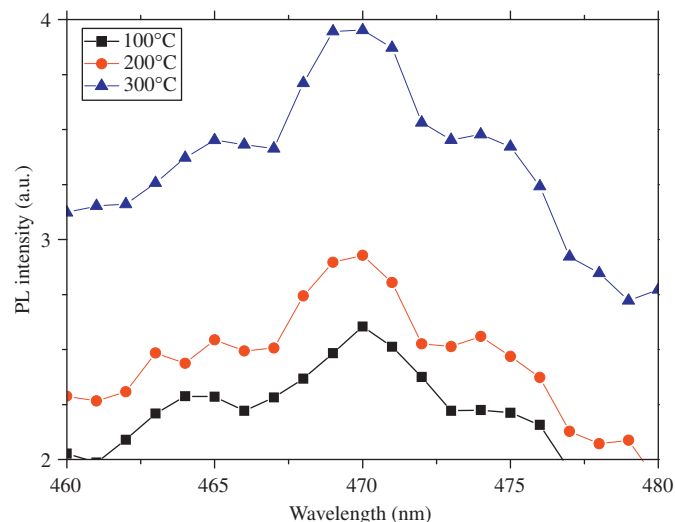


Fig. 7. The PL emission from the ZnS nanoparticles dissolved in methanol under UV light excitations and heat treated at 100 °C, 200 °C and 300 °C respectively for 1 h.

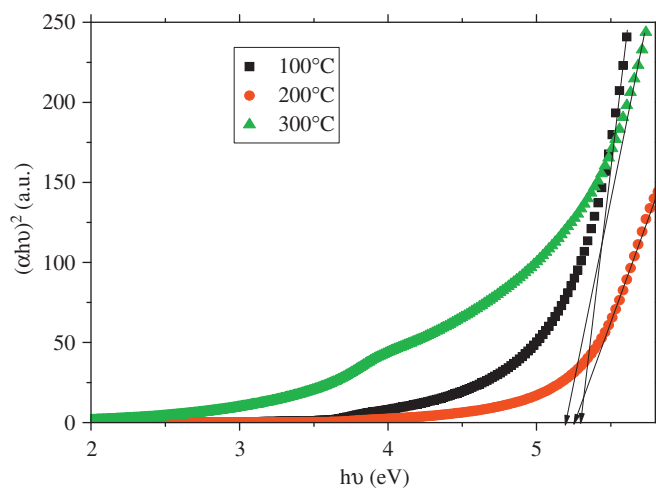


Fig. 6. Calculation of optical band gap from the UV-vis-NIR absorption spectra heat treated at 100 °C, 200 °C and 300 °C respectively for 1 h.

conduction band, can be used to determine the value of the optical band gap of the synthesized ZnS nanoparticles.

The relation between the incident photon energy ($h\nu$) and the absorption coefficient (α) is given by the following relation:

$$(\alpha h\nu)^{1/n} = A(h\nu - E_g) \quad (3)$$

where A is constant and E_g is the band gap of material and the exponent n depends on the type of transition. For direct allowed transition $n=1/2$, for indirect allowed transition $n=2$, for direct forbidden $n=3/2$ and for indirect forbidden $n=3$. Direct band gap of the samples are calculated by plotting $(\alpha h\nu)^2$ vs. $h\nu$ and then extrapolating the straight portion of the curve on $h\nu$ axis at $\alpha=0$, shown in Fig. 6. The optical band gaps of the sample are calculated and found in the range 5.30, 5.25, 5.20 eV for ZnS heat treated at 100 °C, 200 °C and 300 °C

respectively for 1 h. Optical band gap energy of ball milled samples decreases continuously with increasing heat treatment temperature.

The obtained values of the band gap of ZnS nanoparticles are higher than that of the bulk value of ZnS (3.68 eV). This blueshift of the band gap takes place because of the quantum confinement effect [20].

3.4. Photoluminescence study of ZnS nanoparticles

Photoluminescence (PL) of ZnS samples dispersed in methanol has been measured at room temperature. The PL spectrum of ZnS nanoparticles is shown in Fig. 7.

In this work we observed that PL intensity is increasing with heat treatment temperature and the peaks are shifted towards the higher wavelength. In PL process an electron from the ZnS valence band is excited to conduction band and photo-excited electron decay by a recombination process to defects states. The PL emission band with multiple peak maxima indicates the involvement of different luminescence centers in the radiative process. PL spectrum shows the efficient emission of blue color light with peaks at ~ 463 , ~ 465 , ~ 470 , ~ 475 and ~ 479 nm for ZnS heat treated at 100–300 °C for 1 h with excitation wavelength of 280 nm for all samples.

4. Conclusion

Here we have reported the optical properties of ZnS nanoparticles of crystallite size 7–9 nm using mechano-chemical method at room temperature. This method is simpler and suitable for industrial application as it can produce large amount of materials at an ambient temperature in short duration of time and it is a low cost process. The band gap energy of the samples is found in the range 5.2–5.3 eV. PL emissions have been observed under the

same UV light excitation for all samples. PL spectrum shows the efficient emission of blue color light under excitation wavelength of 280 nm.

Acknowledgments

One of the authors (CSP) acknowledges to the MHRD, Government of India for the partial financial support and the Institute Instrumentation Centre of Indian Institute of Technology, Roorkee for providing lab facility.

References

- [1] Xiaosheng Fang, Tianyou Zhai, Ujjal K. Gautam, Liang Li, Limin Wu, Yoshio Bando, Dmitri Golberg, ZnS nanostructures: from synthesis to applications, *Progress in Materials Science* 56 (2011) 175–287.
- [2] R. Rosetti, R. Hull, J.M. Gibson, L.E. Brus, Excited electronic states and optical spectra of ZnS and CdS crystallites in the ~ 15 Å to 50 Å range: evolution from molecular to bulk semiconducting properties, *Journal of Chemical Physics* 82 (1985) 552.
- [3] L. Brus, Electronic wavefunctions in semiconductor clusters, *Journal of Physical Chemistry* 90 (1986) 2555.
- [4] A. Henhlin, Small-particle research: physicochemical properties of extremely small colloidal metal and semiconductor particles, *Chemical Reviews* 89 (1989) 89.
- [5] Y. Wang, N. Herron, Nanometer-sized semiconductor clusters: materials synthesis, quantum size effects, and photophysical properties, *Journal of Physical Chemistry* 95 (1991) 525.
- [6] H. Weller, Colloidal semiconductor Q-particles: chemistry in the transition region between solid state and molecules, *Angewandte Chemie, International Edition (English)* 32 (1993) 41.
- [7] A.P. Alivisatos, Perspectives on the physical chemistry of semiconductor nanocrystals, *Journal of Physical Chemistry* 100 (1996) 13226.
- [8] L. Amirav, A. Amirav, E. Lifshitz, A spray-based method for the production of semiconductor nanocrystals, *Journal of Physical Chemistry Letters* B 109 (2005) 9857.
- [9] T. Tsuzuki, J. Ding, P. McCormick, Mechanochemical synthesis of ultrafine zinc sulphide particles, *Physica B* 239 (1997) 378–387.
- [10] P. Balaz, E. Boldizarova, E. Godocikova, Briancin, Mechanochemical route for sulphide nanoparticles preparation, *Journal of Materials Letters* 57 (2003) 1585.
- [11] S. Sain, S.K. Pradhan, Mechanochemical solid state synthesis of $(\text{Cd}_{0.8}\text{Zn}_{0.2})\text{S}$ quantum dots: microstructure and optical characterizations, *Journal of Alloys and Compounds* 509 (2011) 4176–4184.
- [12] J.F. Xu, H.S. Jiw, Y.W. Tang, Du, Preparation of ZnS nanoparticles by ultrasonic radiation method, *Applied Physics A* 66 (1998) 639.
- [13] S.K. Mandal, A.R. Mandal, S. Das, B. Bhattacharjee, Strong excitonic confinement effect in ZnS and ZnS:Mn nanorods embedded in polycarbonate membrane pores, *Journal of Applied Physics* 101 (2007) 114315.
- [14] C.S. Pathak, M.K. Mandal, Optical properties of Mn^{2+} doped ZnS nanoparticles, *Asian Journal of Chemistry* 23 (10) (2011) 4655–4658.
- [15] S.W. Lu, B.I. Lee, Z.L. Wang, W. Tong, B.K. Wagner, W. Park, C.J. Summers, Synthesis and photoluminescence enhancement of Mn^{2+} -doped ZnS nanocrystals, *Journal of Luminescence* 92 (2001).
- [16] Yanbin Tong, Zijiang Jiang, Cheng Wang, Yi Xin, Zonghao Huang, Sidong Liu, Chunbo Li, Effect of annealing on the morphology and properties of ZnS:Mn nanoparticles/PVP nanofibers, *Materials Letters* 62 (2008) 3385–3387.
- [17] M.M. Biggs, O.M. Ntwaeaborwa, J.J. Terblans, H.C. Swart, Characterization and luminescent properties of $\text{SiO}_2\text{:ZnS:Mn}^{2+}$ and ZnS:Mn^{2+} nanophosphors synthesized by a sol–gel method, *Physica B* 404 (2009) 4470–4475.
- [18] E. Ivanov, C. Suryanarayana, Materials and process design through mechanochemical routes, *Journal of Materials Synthesis and Processing* 8 (nos. 3/4) (2000) 235–244.
- [19] P. Balaz, P. Pourghahramani, E. Dutkova, E. Turianicova, J. Kovac, A. Satka, Mechanochemistry in preparation of nanocrystalline semiconductors, *Physica Status Solidi C* 5 (no. 12) (2008) 3756–3758.
- [20] R.N. Bhargava, D. Gallagher, X. Hong, A. Nurmikko, Optical properties of manganese doped nanocrystals of ZnS, *Physical Review Letters* 72 (1994) 416.